International Journal of Engineering Science 73 (2013) 17–32

Contents lists available at ScienceDirect

International Journal of Engineering Science

journal homepage: www.elsevier.com/locate/ijengsci

Second-order elasticity of soft multilayer capsules: Universal relations and parametric studies

Dong Wang, Mao S. Wu *

School of Mechanical and Aerospace Engineering, Nanyang Technological University, Singapore

ARTICLE INFO

Article history:
Received 7 August 2012
Received in revised form 23 July 2013
Accepted 7 August 2013
Available online 6 September 2013

Keywords:
Multilayer gels
Second-order elasticity
Dilatations
Universal relations

ABSTRACT

Composite gels are of key interest in bioengineering, e.g., as replacement tissues and substrates for stem cell cultures. Although gel elasticity plays a pivotal role in many bio-functions, there is insufficient knowledge on the effect of elastic nonlinearity, multilayer configuration and chemical concentration. To address such issues, multilayer capsules subjected to dilatation fluctuations are investigated using second-order elasticity, validated by universal curves for uniaxial tension and swelling of homogeneous gels. Detailed simulations show that the material inhomogeneity, elastic nonlinearity, shell thicknesses and fluctuation profile all have significant influence on the elastic fields, and hence may be selected to induce favorable microenvironment such as a tensile or compressive stress state appropriate for the targeted functionalities.

1. Introduction

Many biological processes are significantly influenced by mechanical forces. Recent works have shown that stem cell lineage specification, morphology, proliferation, adhesion, apoptosis and other properties are extremely sensitive to the elasticity of the cell microenvironment. For instance, human mesenchymal stem cells (hMSCs) cultured on polyacrylamide gels mimicking the elasticity of brain, muscle and osteoid collagen indicated the greatest expression of neurogenic, myogenic and osteogenic transcripts on these gels, respectively (Engler, Sen, Sweeney, & Discher, 2006). Increased proliferation of hMSCs was also observed on the stiffer methacrylated hyaluronic acid hydrogels as compared to the softer ones over the stiffness range of 3–100 kPa (Marklein & Burdick, 2010). Similarly, the gradient elasticity of photodegradable hydrogels was shown to influence the differentiation of valvular interstitial cells into myofibroblasts (Kloxin, Benton, & Anseth, 2010). The substrate stiffness was also shown to influence the phenotype of embryonic chicken cardiac myocytes, a conclusion reached by culturing the myocytes on laminin-coated polyacrylamide substrates with stiffness in the range of 1–50 kPa (Bajaj, Tang, Saif, & Bashir, 2010). The contractile stress of the cardiac myocytes also increases with the substrate stiffness. These and other investigations have established that elasticity mechanics should be taken into consideration when designing biomaterials. Hydrogels with stiffness varying over several orders of magnitude can be realized by varying the degree of cross-linking and by photochemical modulation (Kloxin et al., 2010; Marklein & Burdick, 2010).

In a recent work, the differentiation of stem cells into bone cells using polymeric multilayer capsules (PMLCs) consisting of alternating layers of poly-L-lysine and poly-L-glutamic acid was demonstrated in vivo (Facca et al., 2010). The polyelectrolyte multilayer films were embedded with bone morphogenetic proteins and transforming growth factors. In general, drugs, nucleic acids, proteins and peptides of various concentrations can be encapsulated within the capsule cores or embedded within the polymer layers (Cortez et al., 2006; Johnston, Cortez, Angelatos, & Caruso, 2006). The PMLCs are usually

* Corresponding author. Address: 50 Nanyang Avenue, Singapore 639798, Singapore. Tel.: +65 6790 5545.
E-mail addresses: dwang2@e.ntu.edu.sg (D. Wang), mmswu@ntu.edu.sg (M.S. Wu).

0020-7225/$ - see front matter © 2013 Elsevier Ltd. All rights reserved.
http://dx.doi.org/10.1016/j.ijengsci.2013.08.001

fabricated by a layer-by-layer technique in which polymers are sequentially adsorbed onto spherical substrates with dimensions ranging from ~10 nm to >10 μm. The multilayer configuration offers advantages in that multiple physico-chemical properties and functions may be achieved within a single coherent material (Detzel, Larkin, & Rajagopalan, 2011; Johnson, DeForest, Pendurti, Anseth, & Bowman, 2010; Teramura, Kaneda, & Iwata, 2007). Furthermore, many biological tissues such as cardiac muscles are multilayered. Hence, for applications in regenerative medicine it may be inherently advantageous to develop biomimicking materials which are similarly multilayered.

The review above emphasizes that mechanical properties play an essential role in the biomaterial design of multilayer capsules for applications in drug delivery, stem cell technology and regenerative medicine. Such diverse applications have motivated our investigation into the elasticity of multilayer capsules. However, in many previous works soft materials are characterized by linear rather than nonlinear elasticity. The stresses and displacements, which have a direct bearing on the biological processes, remain to be studied in detail. Also, the multilayer nature of many soft materials has yet to be considered analytically. The effect of the chemical concentrations of proteins, growth factors, etc. on the mechanical response of the hydrogels has likewise received little attention, although the authors and their associates have initiated research in this area for homogeneous and bilayer capsules (Wang & Wu, 2013; Wu & Kirchner, 2010, 2011).

Much theoretical work on the elasticity of soft materials has been done by the mechanics community, e.g., the third- and fourth-order incompressible elasticities of biological soft tissues (Destrade, Gilchrist, & Ogden, 2010; Hamilton, Ilinskii, & Zabolotskaya, 2004), the instability of an elastic shell modeled as an incompressible Neo-Hookean solid (Goriely & Ben Amar, 2005), the electric field-induced displacement of a charged spherical colloid in a linear elastic compressible hydrogel (Wang & Hill, 2008), and the simulation of tumor growth in its microenvironment, accounting for factors such as nutrient transport, cellular velocity, proliferation and mechanical pressure (Macklin & Lowengrub, 2007). Others have investigated non-affine deformations of polymer gels, as opposed to affine deformations in which the microscopic and macroscopic strains are the same (Wen, Basu, Janmey, & Yodh, 2012). However, little work has been reported on the mechanics of multilayer soft hydrogels, which form a large class of natural and bio-inspired materials.

In this paper, it is intended to study the stresses and displacements in a multilayer hydrogel subjected to various dilatation profiles arising from chemical concentrations. Second-order elasticity (also classified as third-order since the energy density is third order in the strains) is adopted in this study since it represents the next level of complexity beyond first-order or linear elasticity. This choice is also motivated by the availability of analytical solutions which can be readily used for parametric studies with little computational cost. Alternative nonlinear elastic models such as various modifications of the Neo-Hookean model and microstructurally-based models may also be used, but more extensive numerical computations are expected. We also restrict our investigation to elasticity and neglect other effects such as viscoelasticity.

The paper is organized into the following sections. In Section 2, the second-order elastic model is reviewed, and new solutions for multilayer spherical and cylindrical capsules are presented. In Section 3, the second-order elasticity is validated against experimental data for a diverse range of synthetic and biological gels subjected to uniaxial tensile loading and swelling under different pH values. In Section 4, the multilayer solutions are presented and parametric studies are conducted to investigate the dependence of the mechanical response on the gel elasticity, the multilayer configuration, and the dilatation profile. Further discussion is made in Section 5, and a set of concluding remarks is given in Section 6.

2. Solutions for multilayer capsules in second-order elasticity

The second-order elastic theory was developed by Murnaghan (1951), who gave analytical solutions for the loading cases of uniaxial tension, simple shear and torsion of bars and the compression of spherical shells and cylindrical tubes. This (Wang & Wu, 2013; Wu & Kirchner, 2010, 2011) and other higher-order elasticity theories (Destrade et al., 2010; Hamilton et al., 2004) have recently been employed for the investigation of biological gels. In the following, it is first shown that the previously obtained analytical solutions for uniaxial tensile loading of soft gels can be recast into a universal form when certain modified stress and strain parameters are defined. Subsequently, the governing field equations for multilayer spherical and cylindrical capsules subjected to a stepped dilatation profile are solved, yielding analytical expressions for the stresses and displacements. It is also shown specifically that a universal form for the displacement (and hence swelling) solution can be obtained if a modified pH parameter is defined. Experimental data are fitted against these universal relations.

As a starting point, higher-order elasticities employ a strain energy density W of the invariants of the Green–Lagrange strain $\mathbf{E}$ (Destrade et al., 2010). The choice of invariants can be $I_1 = \mathrm{tr}\,\mathbf{E}$, $I_2 = [(\mathrm{tr}\,\mathbf{E})^2 - \mathrm{tr}(\mathbf{E}^2)]/2$ and $I_3 = \det\mathbf{E}$. In second-order compressible elasticity, W is expanded as a linear combination of the invariants up to the third order in the strains, i.e.:

$$W = \frac{\lambda + 2\mu}{2} I_1^2 - 2\mu I_2 + \frac{l + 2m}{3} I_1^3 - 2mI_1 I_2 + nI_3, \tag{1}$$

where λ, μ are the second-order and l, m and n the third-order elastic constants, respectively (Murnaghan, 1951). A total of five elastic constants are thus needed. Other choices of W may be employed, e.g., W for third-order incompressible isotropic elasticity (Hamilton et al., 2004).

2.1. Uniaxial tension

Consider an isotropic homogeneous cylindrical bar under a uniaxial tensile stress σ, defined as the applied force per unit initial cross-sectional area (engineering stress). Using a perturbation analysis, the engineering strain ε takes the form:

$$\varepsilon = \frac{\sigma}{E} + \delta\left(\frac{\sigma}{E}\right)^2, \tag{2}$$

where E is the Young's modulus related to λ and μ via the well-known relation

$$E = \frac{\mu(3\lambda + 2\mu)}{\lambda + \mu}, \tag{3}$$

and δ is dimensionless and related to the five elastic constants

$$\delta = -\frac{3}{2} - \frac{\mu^2 l}{(3\lambda + 2\mu)(\lambda + \mu)^2} - \frac{(3\lambda + 2\mu)}{2(\lambda + \mu)^2} m - \frac{3\lambda^2}{4\mu(3\lambda + 2\mu)(\lambda + \mu)} n. \tag{4}$$

The details of the derivation of Eqs. (2)–(4) can be found in the original work of Murnaghan (1951). Eq. (2) contains two parameters E and δ (rather than five), implying that different values of the five elastic constants can lead to the same stress–strain response provided they share the same values of E and δ according to Eqs. (3) and (4). Moreover, δ can be positive or negative. A negative value implies a nonlinear stiffening effect as the stress produces a strain less than that predicted by linear elasticity. Conversely, a positive δ implies a softening effect.

Multiplying Eq. (2) by δ and defining a modified strain $\tilde{\varepsilon} = \delta\varepsilon$ and a modified (dimensionless) stress $\tilde{\sigma} = \delta\sigma/E$, the following simple universal relation is obtained:

$$\tilde{\varepsilon} = \tilde{\sigma} + \tilde{\sigma}^2, \tag{5}$$

where no material parameters appear explicitly. The values of E and δ can be obtained by fitting Eq. (2) against the stress–strain data, and can be used to calculate the modified strain and stress. The modified $\tilde{\sigma}$ vs. $\tilde{\varepsilon}$ data can be compared to the universal form of Eq. (5). A universal representation is a convenient way to collapse different data sets into a single reduced data set, as illustrated in Section 3.

2.2. Dilatation loading of multilayer spherical and cylindrical capsules

Consider next an N-layer spherical (or cylindrical) capsule subjected to a fluctuating spherically (or radially) symmetric dilatation profile (Fig. 1). The interfaces are located at the radial coordinates $r = r_j$, $j = 1, N$. The layers are nonlinearly elastic, isotropic, homogeneous and perfectly bonded to one another, but can be of dissimilar material compositions and thicknesses. Fluctuations such as the chemical concentration $c(r)$ result in local dilatation field $\vartheta(r)$, e.g., the stepped profiles ϑ_{p1} and ϑ_{p2} indicated in Fig. 1. The relation between c and ϑ is given by the change in lattice parameter per unit concentration and depends on the specific polymer gel and the chemical species. An analogous relation exists between temperature and dilatation, in which the change in thermal strain per unit temperature is defined by the coefficient of thermal expansion. For the elasticity problem, however, it is not necessary to specify this relation and $\vartheta(r)$ enters the governing equation directly. In general, the fluctuation field may be controlled, as in the embedding of drugs, nucleic acids, nutrients and growth factors of selected concentrations within the layers of sub-micrometer thicknesses (Cortez et al., 2006; Facca et al., 2010; Johnston et al., 2006).

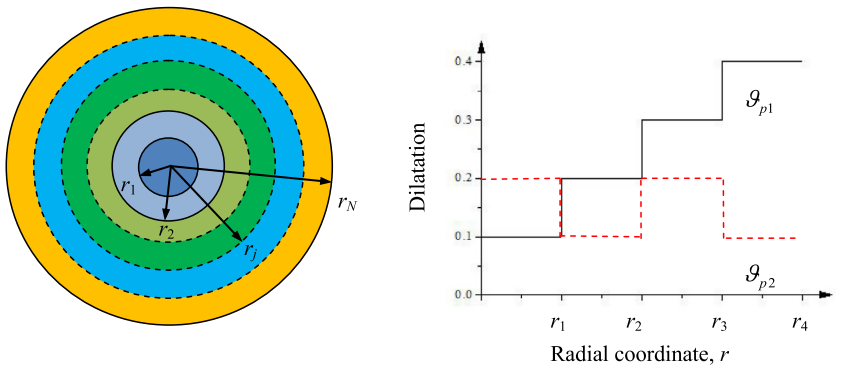

Fig. 1. A spherical or cylindrical hydrogel composite consisting of N layers, with core radius r_1 and outermost radius r_N. Two stepped dilatation profiles ϑ_{p1} and ϑ_{p2} in a four-layer composite are shown on the right.

A total of five elastic constants λ_j, μ_j, l_j, m_j and n_j, $j = 1, N$ are needed to describe the elasticity of each layer j. The dilatation is effectively treated as the loading associated with a body force density (Wang & Wu, 2013; Wu & Kirchner, 2010, 2011). The governing equilibrium equation in the radial direction can be written as:

$$T_r' + \frac{2}{r}T_r - \frac{2}{r}T_\theta = k\left(\lambda + \frac{2}{3}\mu\right)\frac{d(3\vartheta)}{dr} - k^2\left(\lambda + \frac{2}{3}\mu - 2l - \frac{2n}{9}\right)(3\vartheta)\frac{d(3\vartheta)}{dr}, \tag{6}$$

for multilayer spheres, where T_r and T_θ are the radial and meridional stresses (the azimuthal component $T_\phi = T_\theta$ for spherically symmetric loading) in a spherical coordinate (r, θ, ϕ) system, and

$$T_r' + \frac{1}{r}T_r - \frac{1}{r}T_\varphi = k\left(\lambda + \frac{2}{3}\mu\right)\frac{d(3\vartheta)}{dr} - k^2\left(\lambda + \frac{2}{3}\mu - 2l - \frac{2n}{9}\right)(3\vartheta)\frac{d(3\vartheta)}{dr}, \tag{7}$$

for multilayer cylinders, where T_r and T_φ are the radial and circumferential stresses in a cylindrical coordinate (r, φ, z) system. The prime denotes differentiation with respect to r, and k and k^2 keep track of the order of approximation (Murnaghan, 1951). For convenience, the subscripts of the elastic constants indicating the layers are dropped. Eqs. (6) and (7) can be transformed into equations involving the radial displacement u_r. Specifically, the stresses are derived from W via the relation

$$\mathbf{T} = \mathbf{J}(\partial W/\partial \mathbf{E}), \tag{8}$$

where $\mathbf{T}$ is the matrix of stresses and $\mathbf{J}$ is the matrix relating current to reference coordinates. For multilayer spheres with spherically symmetric loading, $\mathbf{J}$ and $\mathbf{E}$ are 3×3 diagonal matrices:

$$\mathbf{J} = \operatorname{diag}\left[1 + ku_r', 1 + \frac{ku_r}{r}, 1 + \frac{ku_r}{r}\right], \tag{9}$$

$$\mathbf{E} = \frac{1}{2}(\mathbf{J} * \mathbf{J} - \mathbf{I}) = k\ \operatorname{diag}\left[u_r', \frac{u_r}{r}, \frac{u_r}{r}\right] + \frac{1}{2}k^2\ \operatorname{diag}\left[u_r'^2, \frac{{u_r}^2}{r^2}, \frac{{u_r}^2}{r^2}\right], \tag{10}$$

where $\mathbf{I}$ is the identity matrix and $*$ denotes the transpose. For multilayer cylinders with radially symmetric loading, they are 2×2 diagonal matrices:

$$\mathbf{J} = \operatorname{diag}\left[1 + ku_r', 1 + \frac{ku_r}{r}\right], \tag{11}$$

$$\mathbf{E} = k\ \operatorname{diag}\left[u_r', \frac{u_r}{r}\right] + \frac{1}{2}k^2\ \operatorname{diag}\left[u_r'^2, \frac{{u_r}^2}{r^2}\right]. \tag{12}$$

The cylinder problem is essentially a plane problem. By the perturbation procedure, u_r is decomposed into a linear (u) and a nonlinear (w) part such that $u_r = u + kw$, where k keeps track of the order of approximation. The total displacement is the simple sum of u and w. By Eq. (8), the stress components can be expressed in terms of u and w, resulting in $T_r = kT_r^L + k^2T_r^{NL}$, where T_r^L and T_r^{NL} denote the linear and nonlinear components of the radial stress, respectively, and similarly for T_θ and T_φ. The stresses are the simple sums of their respective linear and nonlinear parts. For multilayer spheres, Eq. (6) separates into two parts, associated with k and k^2, respectively:

$$\frac{d}{dr}\left[\frac{1}{r^2}\frac{d(r^2u)}{dr}\right] = L\frac{d\vartheta}{dr}, \quad L = \frac{3\lambda + 2\mu}{\lambda + 2\mu}, \tag{13}$$

$$\begin{aligned}(\lambda + 2\mu)\left(w'' + 2\frac{w'}{r} - 2\frac{w}{r^2}\right) &= -2(\lambda + 3\mu + 2m)\left[\left(u'' + 2\frac{u'}{r} - 2\frac{u}{r^2}\right)u' - \frac{1}{r}\left(u' - \frac{u}{r}\right)^2\right] \\ &\quad - (\lambda + 2l)\left(u'' + 2\frac{u'}{r} - 2\frac{u}{r^2}\right)\left(u' + 2\frac{u}{r}\right) - \left(\lambda + \frac{2}{3}\mu - 2l - \frac{2n}{9}\right)9\vartheta\frac{d\vartheta}{dr}.\end{aligned} \tag{14}$$

For multilayer cylinders, Eq. (7) similarly separates into two parts:

$$u'' + \frac{u'}{r} - \frac{u}{r^2} = L\frac{d\vartheta}{dr}, \tag{15}$$

$$\begin{aligned}(\lambda + 2\mu)\left(w'' + \frac{w'}{r} - \frac{w}{r^2}\right) &= -2(\lambda + 3\mu + 2m)\left(u'u'' + \frac{1}{2r}u'^2 - \frac{u^2}{2r^3}\right) - (\lambda + 2l)\left(u'' + \frac{u'}{r} - \frac{u}{r^2}\right)\left(u' + \frac{u}{r}\right) \\ &\quad - \left(\lambda + \frac{2}{3}\mu - 2l - \frac{2n}{9}\right)9\vartheta\frac{d\vartheta}{dr}.\end{aligned} \tag{16}$$

Eqs. (13) and (15) are the classical equilibrium equations for linear thermoelasticity, if ϑ is interpreted as the dilatation due to thermal expansion. Mathematically, they are second-order differential equations with the unknowns u and w.

Assume that ϑ_{p1} or ϑ_{p2} is represented by the constants ϑ_j, $j = 1, N$. Solving Eqs. (13) and (14) for each layer in spherical coordinates and Eqs. (15) and (16) for each layer in cylindrical coordinates, the displacements u_j and w_j, $j = 1, N$ can be obtained in analytical form:

$$u_j = A_j r + \frac{B_j r_{j-1}^3}{r^2}, \quad w_j = C_j r + \frac{D_j r_{j-1}^3}{r^2} + \frac{\lambda_j + 3\mu_j + 2m_j}{\lambda_j + 2\mu_j} B_j^2 \frac{r_{j-1}^6}{r^5}, \quad 1 \le j \le N, \tag{17}$$

for multilayer spheres, and

$$u_j = A_j r + \frac{B_j r_{j-1}^2}{r}, \quad w_j = C_j r + \frac{D_j r_{j-1}^2}{r} + \frac{(\lambda_j + 3\mu_j + 2m_j)}{2(\lambda_j + 2\mu_j)} B_j^2 \frac{r_{j-1}^4}{r^3}, \quad 1 \le j \le N, \tag{18}$$

for multilayer cylinders, where $B_1 = D_1 = 0$ and there remain $4N - 2$ unknown dimensionless parameters A_1, C_1, and A_j, B_j, C_j, D_j, $j = 2, N$. It should be noted that A_j, B_j, C_j, D_j for spheres and cylinders are different. These parameters depend on $\lambda_j, \mu_j, l_j, m_j, n_j$, the layer thicknesses $r_j - r_{j-1}$, $j = 1, N$ (the inner radius of the core $r_0 = 0$) and the dilatation ϑ_j. Using Eq. (8), the linear and nonlinear components of the radial and meridional stresses for multilayer spheres in each layer j can be written as:

$$T_{rj}^L = (A_j - \vartheta_j)\left(3\lambda_j + 2\mu_j\right) - 4B_j\mu_j \frac{r_{j-1}^3}{r^3}, \tag{19}$$

$$T_{\theta j}^L = (A_j - \vartheta_j)\left(3\lambda_j + 2\mu_j\right) + 2B_j\mu_j \frac{r_{j-1}^3}{r^3}, \tag{20}$$

$$T_{rj}^{NL} = \frac{1}{2(\lambda_j + 2\mu_j)r^6}(H_{1j} + H_{2j}r^3 + H_{3j}r^6), \tag{21}$$

$$T_{\theta j}^{NL} = \frac{1}{2\left(\lambda_j + 2\mu_j\right)r^6}\left(-2H_{1j} - H_{2j}\frac{r^3}{2} + H_{3j}r^6\right), \tag{22}$$

where H_{1j}, H_{2j} and H_{3j} are parameters related to A_j, B_j, C_j, D_j for multilayer spheres. For multilayer cylinders, the linear and nonlinear components of the radial and circumferential stresses in each layer j can be written as:

$$T_{rj}^L = 2(\lambda_j + \mu_j)(A_j - \vartheta_j) - 2B_j\mu_j \frac{r_{j-1}^2}{r^2}, \tag{23}$$

$$T_{\varphi j}^L = 2(\lambda_j + \mu_j)(A_j - \vartheta_j) + 2B_j\mu_j \frac{r_{j-1}^2}{r^2}, \tag{24}$$

$$T_{rj}^{NL} = \frac{1}{(\lambda_j + 2\mu_j)r^4}(H_{1j} + H_{2j}r^2 + H_{3j}r^4), \tag{25}$$

$$T_{\varphi j}^{NL} = \frac{1}{(\lambda_j + 2\mu_j)r^4}(-3H_{1j} - H_{2j}r^2 + H_{3j}r^4), \tag{26}$$

where H_{1j}, H_{2j} and H_{3j} are parameters related to A_j, B_j, C_j, D_j for multilayer cylinders. Eqs. (17)–(26) are all power-law expressions. To solve for the $4N - 2$ parameters, the continuity of u_r across the interfaces at r_j, $j = 1, N - 1$ requires $u_j(r_j) = u_{j+1}(r_j)$, $w_j(r_j) = w_{j+1}(r_j)$, while the continuity of T_r at the same interfaces requires $T_{r_j}^L(r_j) = T_{r_{j+1}}^L(r_j)$, $T_{r_j}^{NL}(r_j) = T_{r_{j+1}}^{NL}(r_j)$, and finally the traction-free condition at the outermost surface requires $T_{r_N}^L(r_N) = T_{r_N}^{NL}(r_N) = 0$ for both multilayer spheres and cylinders. These constitute a set of $4N - 2$ equations which permit the solution for the same number of parameters. The expressions for the constants H_{1j}, H_{2j} and H_{3j} in terms of the elastic constants, the thicknesses and the dilatations are rather cumbersome and are omitted here for brevity.

3. Universal curves and experimental data

3.1. Uniaxial tension

The universal relation of Eq. (5) for uniaxial tension is validated against fourteen data sets labeled 1–14 in Table 1. The materials include biopolymer networks (neurofilaments, collagen, vimentin, fibrin and actin) (Storm, Pastore, MacKintosh, Lubensky, & Janmey, 2005), covalently crosslinked networks based on poly(propylene glycol) bis(aceto-acetate) with either neopentyl glycol diacrylate (PPG BisAcAc-NPGDA) or with 2-hydroxyethyl acrylate derivatized bis(4-isocyanatocyclohexyl) methane (PPG BisAc-Ac-EA-HMDI-EA) (Williams, Mather, Miller, & Long, 2007), extremely soft poly(acrylamide) (PAAm)

Table 1
Elastic parameters E and δ obtained from fitting Eq. (2) to uniaxial tensile test data.

No.	Material	E (kPa)	δ
1	Collagen (Storm et al., 2005)	87.9282	−1.39442
2	Fibrin (steady state) (Storm et al., 2005)	53.0106	−0.6301
3	Fibrin(oscillator) (Storm et al., 2005)	124.561	−0.3108
4	Actin (Storm et al., 2005)	346.669	−1.60691
5	PPG BisAcAc NPGDA network (Williams, Mather, Miller, & Long, 2007)	96.4221	0.0426442
6	PPG BisAcAc-EA-HMDI-EA network (Williams, Mather, Miller, & Long, 2007)	643.774	−0.299947
7	$K = 2$, $N_s = 17.88 \pm 7.4$, uniaxial deformation (Dobrynin & Carrillo, 2011)	0.0222387	−0.124757
8	$K = 2$, $N_s = 18.03 \pm 6.7$, uniaxial deformation (Dobrynin & Carrillo, 2011)	0.0607035	−0.133834
9	PAAm-CG-2 (Yohsuke, Urayama, Takigawa, & Ito, 2011)	1.37086	0.163572
10	PAAm-CG-4 (Yohsuke, Urayama, Takigawa, & Ito, 2011)	2.92523	0.128837
11	P-GEL-15 (Urayama, Ogasawara, & Takigawa, 2006)	31.7298	−0.0692103
12	C-GEL-10 (Urayama, Ogasawara, & Takigawa, 2006)	17.1659	0.246195
13	Gels containing 10% gellan polymer with 6 mM Ca++ (Tang, Tung, Lelievre, & Zeng, 1997)	182.349	−1.87775
14	Longitudinal media of human abdominal aorta (Balzani, Neff, Schroder, & Holzapfel, 2006)	52.5559	−0.715767

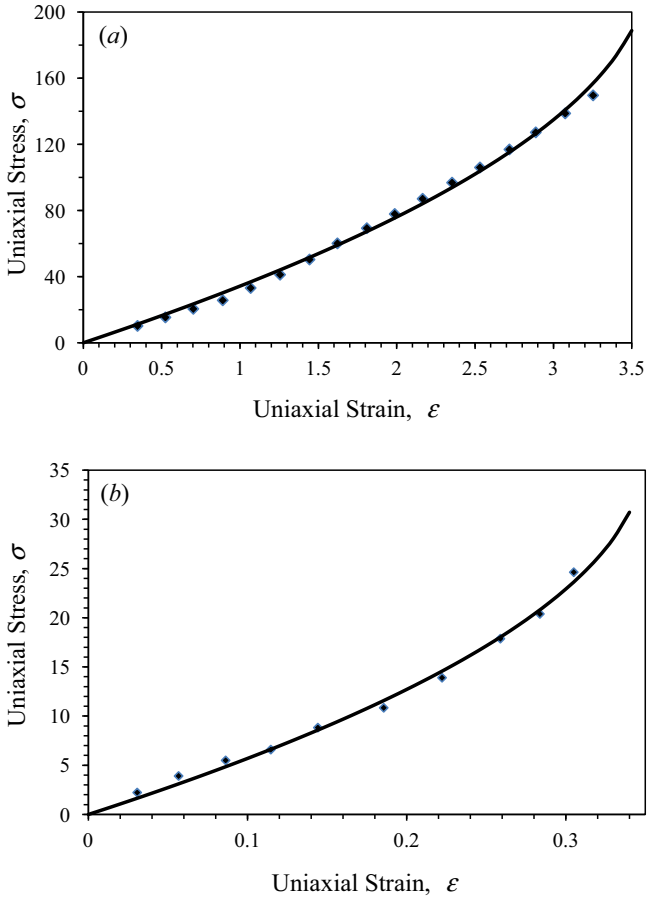

Fig. 2. Uniaxial stress–strain curves of (a) P-GEL-15 polymer networks (Urayama, Ogasawara, & Takigawa, 2006) and (b) human abdominal aorta (Balzani, Neff, Schroder, & Holzapfel, 2006). The lines represent the best fit to the theoretical expression predicted by second-order elasticity.

hydrogels (Yohsuke, Urayama, Takigawa, & Ito, 2011), physical and chemical gels of poly(vinyl alcohol) (Urayama, Ogasawara, & Takigawa, 2006), calcium-crosslinked gellan gels (Tang, Tung, Lelievre, & Zeng, 1997), and a longitudinal strip of human abdominal aorta (Balzani, Neff, Schroder, & Holzapfel, 2006). In addition, molecular dynamics simulations of semiflexible networks (Dobrynin & Carrillo, 2011) are also included in the data sets.

Table 1 lists the materials and the corresponding parameters E and δ obtained through data fitting of Eq. (2). Two examples of $\sigma-\varepsilon$ plot are shown in Fig. 2. Fig. 2(a) shows the curve of Eq. (2) and the test data for a physical gel of poly(vinyl alcohol) (labeled P-GEL-15 in the original paper of Urayama et al. (2006)), while Fig. 2(b) compares Eq. (2) to the data for a

longitudinal strip of human abdominal aorta (Balzani et al., 2006). The value of δ is negative in these two cases, implying a stiffening effect associated with second-order elasticity. Table 1 shows that most of the materials display the stiffening effect, whereas the PPG BisAcAc-NPGDA networks, the soft PAAm gels and the chemical gels of poly(vinyl alcohol) display a softening effect with corresponding positive δ.

Fig. 3 plots the universal relation, i.e., Eq. (5), in the form of $-\tilde{\sigma}$ vs. $-\tilde{\varepsilon}$. It can be seen that the fourteen data sets collapse into a narrow data band, through which the universal line passes. The agreement between the nonlinear elastic model prediction and the data is reasonably good, given that the materials include both biological and synthetic gels of various types. The $\tilde{\sigma}$ vs. $\tilde{\varepsilon}$ behavior is significantly nonlinear and it is insufficient to describe the gel elasticity using only a second-order elastic constant such as E. A universal relation for uniaxial tension has also been derived from a microscopic model of the polymer chains as worm-like chains (Dobrynin & Carrillo, 2011). Fig. 3 shows that a simple second-order elastic continuum model is also capable of describing such a universal relation. Indeed, as the next section shows, a universal relation can also be developed for the swelling behavior.

3.2. Swelling

In this sub-section, the data for the swelling dependence on the pH of homogeneous polymer gels are fitted against a universal relation. The swelling is characterized by the weight ratio Q, defined as the ratio of the mass of water absorbed to the mass of the dry polymer. For spheres,

$$Q = \frac{\rho_{water}[(R+u_r)^3 - R^3]}{\rho_{polymer} R^3} = \frac{\rho_{water}\left[\left(1+\frac{u_r}{R}\right)^3 - 1\right]}{\rho_{polymer}}, \tag{27}$$

while for cylinders,

$$Q = \frac{\rho_{water} h[(R+u_r)^2 - R^2]}{\rho_{polymer} h R^2} = \frac{\rho_{water}\left[\left(1+\frac{u_r}{R}\right)^2 - 1\right]}{\rho_{polymer}}. \tag{28}$$

In the above definitions, ρ_{water} and $\rho_{polymer}$ are the densities of water and polymer, respectively, R is the radius of the gel at dry state, $u_r \equiv u_r(R)$ is the radial displacement at the outermost surface after swelling, and h is the thickness of the cylinder gel.

It can be shown that the parameters A_j, B_j, C_j, Dj in Eqs. (17) and (18) are quadratic functions of the dilatation ϑ_j, after applying the boundary conditions. Thus, u_r/R is a quadratic function of dilatation ϑ_j. For a single-layer homogeneous sphere or cylinder, the following linear (and simplest) assumption is made between the dilatation and pH (which is a logarithmic measure of the concentration of hydrogen ions):

$$\vartheta = a\ \mathrm{pH} + b, \tag{29}$$

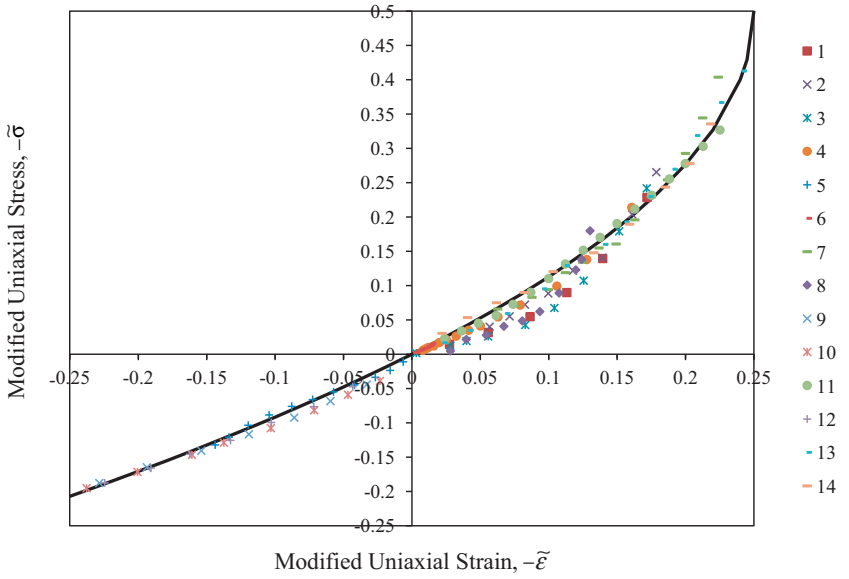

Fig. 3. Dependence of modified stress $-\tilde{\sigma}$ on modified strain $-\tilde{\varepsilon}$. The materials for the data sets 1–14 are listed in Table 1. The solid line represents the universal line.

for the region $0.1R < r < R$, and $\vartheta = 0$ for a small pH-insensitive core $r < 0.1R$. The constants a and b can be obtained through fitting the displacement model to the swelling data. Hence, u_r/R is a quadratic function of pH in the second-order elasticity model:

$$\frac{u_r}{R} = a'\mathrm{pH}^2 + b'\mathrm{pH} + c', \tag{30}$$

where a', b' and c' are parameters related to the elastic constants as well as a and b of Eq. (29). Finally, by Eqs. (27) and (28), the swelling ratio can be written as:

$$Q = \frac{\rho_{water}[(1 + a'\mathrm{pH}^2 + b'\mathrm{pH} + c')^3 - 1]}{\rho_{polymer}}, \tag{31}$$

for spheres and

$$Q = \frac{\rho_{water}[(1 + a'\mathrm{pH}^2 + b'\mathrm{pH} + c')^2 - 1]}{\rho_{polymer}}, \tag{32}$$

for cylinders. Note that Q is either a sextic or a quartic function of pH. By fitting Eqs. (31) and (32) to the swelling data, the parameters a', b', c' can be determined. In a similar way as for the uniaxial tension data, universal relations for Q can be developed. Defining a modified swelling ratio $\tilde{Q} = \rho_{polymer}/\rho_{water} \bullet Q$ and a modified pH $\tilde{P}_h = a'\mathrm{pH}^2 + b'\mathrm{pH} + c'$, Eqs. (31) and (32) can be recast in the following universal forms:

$$\tilde{Q} = (1 + \tilde{P}_h)^3 - 1, \quad \tilde{Q} = (1 + \tilde{P}_h)^2 - 1, \tag{33}$$

where no material parameters appear explicitly. It should be noted that universal relations can be similarly derived for a multilayer capsule, following the steps of Eqs. (29) and (30).

Twenty sets of swelling vs. pH data, labeled 15–34 in Table 2, are used to validate the universal relations. The polymer gels include: styrene and 4-vinylpyridine copolymers (St/4VP copolymers) (Batich, Jun, Bucaria, & Elsabee, 1993), poly(N-isopropylacrylamide-co-sodium acrylate) gels (NIPA/SA) (Motonaga & Shibayama, 2001), poly(ethylene glycol) methyl ether methacrylates-poly(acrylic acid) double-network hydrogels (PPEGMA-PAA) (Naficy, Razal, Whitten, Wallace, & Spinks, 2012), poly(N-isopropylacrylamide-co-acrylic acid) gels (NIPA/AAc) (Shibayama, Ikkai, Inamoto, Nomura, & Han, 1996), polyacrylamide/laponite clay nanocomposite hydrogels (NC) (Li, Kim, Siddaramaiah, & Lee, 2009), poly(methacrylic acid)/Poly(N-isopropylacrylamide) interpenetrating polymer networks (PMAA/PNIPAAm IPN) (Zhang & Peppas, 2000), and hydrophobically modified poly(acrylic acid) gels (HM PAA gels) (Philippova, Hourdet, Audebert, & Khokhlov, 1997).

Table 2 lists the materials tested and the corresponding values for the parameters a', b', c' appearing in Eq. (31) or Eq. (32). The St/4VP copolymers are spherical whereas the rest of the polymers in Table 2 are cylindrical. Fig. 4(a) shows Q vs. pH for the (NIPA/AAc) gels (Shibayama et al., 1996). The weight ratio increases with pH, reaches a peak around a pH value of 8, and decreases with pH thereafter. This non-monotonic Q dependence on pH is fairly well-reproduced by Eq. (32), indicated as a solid curve. In contrast, Fig. 4(b) shows that the weight ratio of HM PAA gels C8–20% (Philippova et al., 1997) increases monotonically with pH up to the value of 9. Here the theoretical prediction of Eq. (32) is acceptable, although the point of inflection is not well-captured.

Table 2
Parameters a', b' and c' obtained from fitting Eqs. (31) and (32) to swelling data.

No.	System	a'	b'	c'
15	St/4VP copolymer (Batich, Jun, Bucaria, & Elsabee, 1993)	−0.0164765	−0.0990889	1.25548
16	St/4VP copolymer (Batich, Jun, Bucaria, & Elsabee, 1993)	−0.0848899	0.298232	0.855509
17	St/4VP copolymer (Batich, Jun, Bucaria, & Elsabee, 1993)	−0.0145595	−0.105732	1.23548
18	NIPA/SA gel (Motonaga & Shibayama, 2001)	−0.0289723	0.481836	−1.16304
19	PPEGMA1100-PAA gel (Naficy et al., 2012)	0.107563	−0.293249	0.795212
20	PPEGMA475-PAA gel (Naficy et al., 2012)	0.0603298	0.108628	−0.107012
21	PAA gel (Naficy et al., 2012)	0.0256669	0.767233	−0.812141
22	NIPA/AAc gels (Shibayama et al., 1996)	−0.0557175	0.917362	−2.52187
23	Polyacrylamide/laponite clay nanocomposite hydrogel NC15 (Li, Kim, Siddaramaiah, & Lee, 2009)	0.0519988	−0.664552	3.68776
24	Polyacrylamide/laponite clay nanocomposite hydrogel NC20 (Li, Kim, Siddaramaiah, & Lee, 2009)	0.0792195	−0.940206	4.46783
25	Polyacrylamide/laponite clay nanocomposite hydrogel NC25 (Li, Kim, Siddaramaiah, & Lee, 2009)	0.119256	−1.30251	5.06215
26	PMAA/PNIPAAm IPN (Zhang & Peppas, 2000)	−0.0204942	0.435262	−0.936233
27	PMAA (Zhang & Peppas, 2000)	−0.0138649	2.2371	−7.39658
28	PAA gel (Philippova, Hourdet, Audebert, & Khokhlov, 1997)	−0.585597	9.82948	−21.667
29	HM PAA gels C8–2.5% (Philippova, Hourdet, Audebert, & Khokhlov, 1997)	−0.675248	11.6895	−31.5438
30	HM PAA gels C8–10% (Philippova, Hourdet, Audebert, & Khokhlov, 1997)	−1.16268	20.9599	−76.6288
31	HM PAA gels C8–20% (Philippova, Hourdet, Audebert, & Khokhlov, 1997)	0.139643	1.61668	−9.73172
32	PAA gels (Philippova, Hourdet, Audebert, & Khokhlov, 1997)	−0.584954	9.84174	−21.7437
33	HM PAA gels C8–5% (Philippova, Hourdet, Audebert, & Khokhlov, 1997)	−0.67579	12.0035	−34.5026
34	HM PAA gels C12–5% (Philippova, Hourdet, Audebert, & Khokhlov, 1997)	−0.37782	7.82808	−22.9672

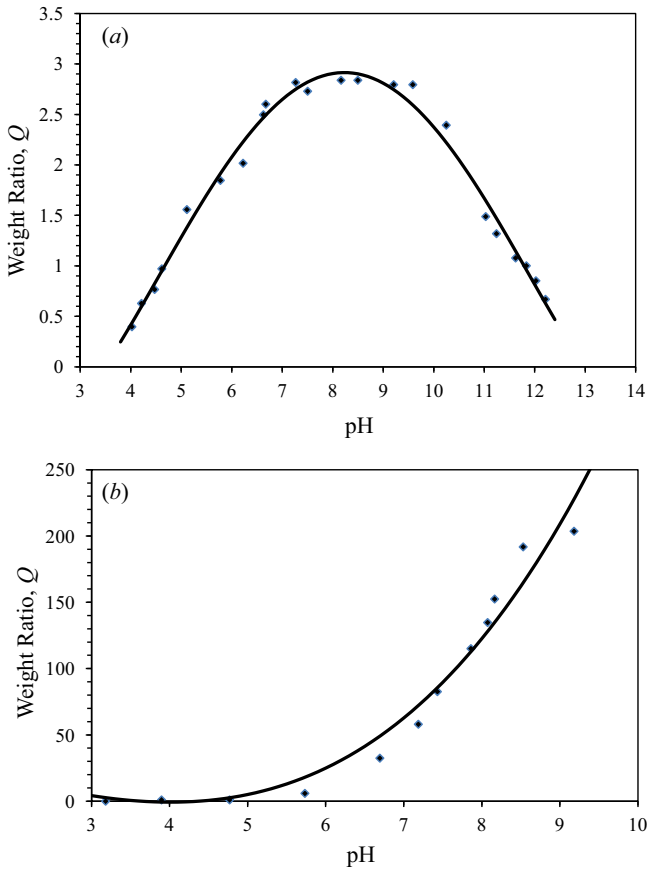

Fig. 4. Dependence of (a) the poly(N-isopropylacrylamide-co-acrylic acid) gels (NIPA/AAc) (Shibayama et al., 1996), and (b) hydrophobically modified poly(acrylic acid) gels (HM PAA C8–20%) (Philippova, Hourdet, Audebert, & Khokhlov, 1997) on pH. The solid lines represent the theoretical fit of the second-order elastic model to the experimental data.

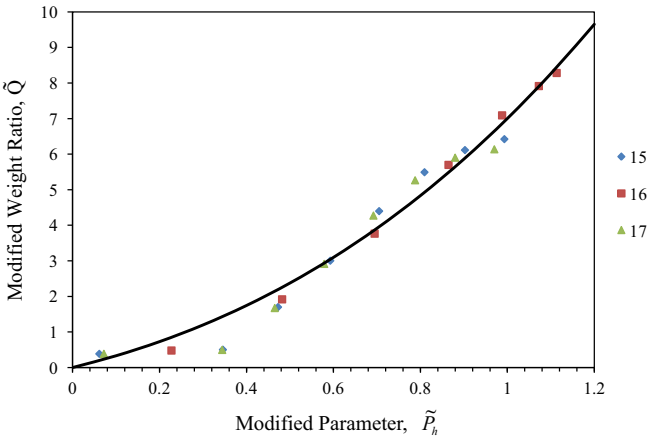

Fig. 5. Dependence of the modified weight ratio ($\tilde{Q}$) due to the swelling of spherical capsules on the modified pH ($\tilde{P}_h$). The materials for the data sets 15–17 are listed in Table 2. The solid line represents the universal line predicted by the second-order elastic model.

Taking $\rho_{polymer}/\rho_{water} \approx 1.4$ (a reasonable estimate for the polymers) and the values of a', b', c' in Table 2 for the different polymers, the modified data can be computed. Fig. 5 plots the modified weight ratio against the modified pH for the case of spherical capsules (Batich et al., 1993). The universal curve predicted by Eq. (33) fits the data reasonably well. Fig. 6 assembles the $\tilde{Q} - \tilde{P}_h$ data for cylindrical capsules in two separate plots for clarity. The upper (a) and lower (b) plots show the data

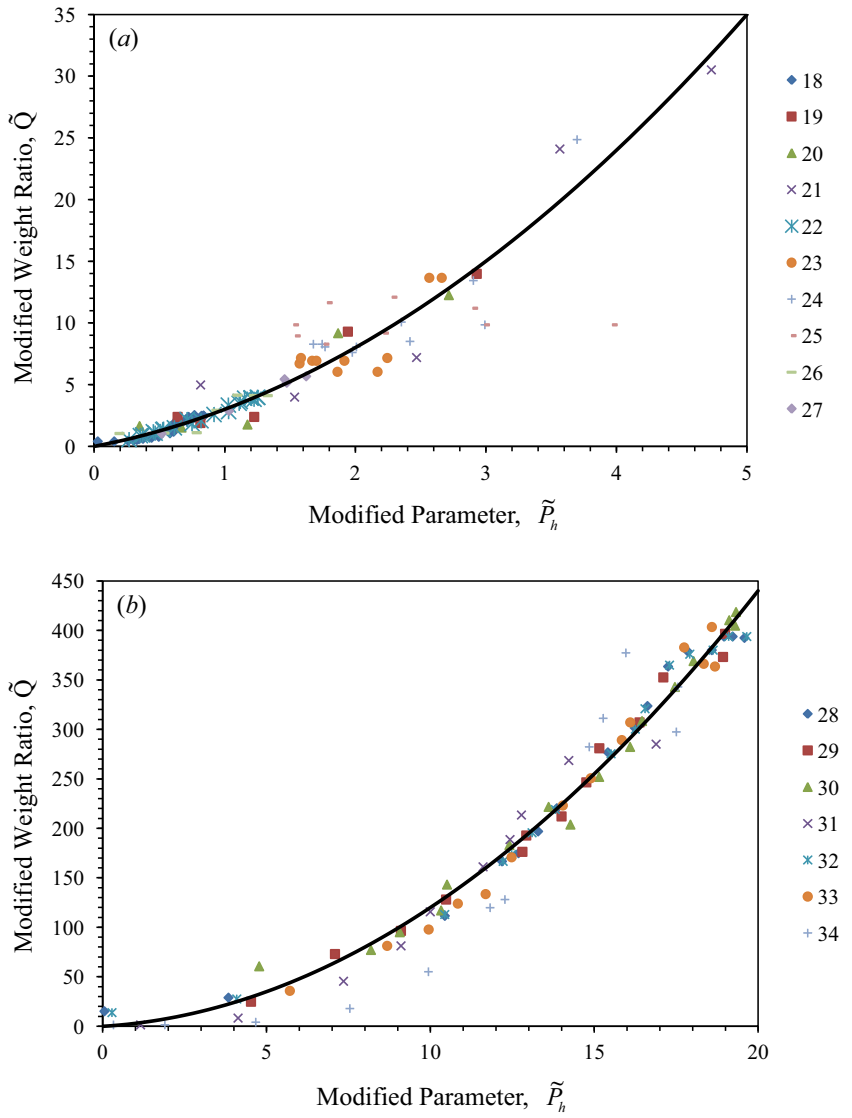

Fig. 6. Dependence of the modified weight ratio ($\tilde{Q}$) due to the swelling of cylindrical capsules on the modified pH ($\tilde{P}_h$). The materials for the data sets 18–27, and those for the data sets 28–34, are listed in Table 2. The solid lines represent the universal line predicted by the second-order elastic model.

labeled 18–27 and 28–34 in Table 2, respectively. The modified pH value in Fig. 6(a) is less than 5, while it is mostly between 4 and 20 in Fig. 6(b). Good agreement is obtained between the reduced data and the universal curve in Fig. 6. Hence, the second-order elastic model captures fairly well the swelling behavior of a diverse range of polymers and composites.

4. Multilayer simulations: parametric studies

On the basis of the second-order elastic model, which has been validated against uniaxial tension and swelling data, theoretical predictions can now be made via simulations for multilayer configurations of polymer gels. Multilayers are gaining increasing importance in the fields of regenerative medicine, stem cell technology and drug delivery, as reviewed in Section 1. Focus will be placed on the influence of the elastic constants, the interface positions and the dilatation profile on the displacement and stresses in spherical multilayers.

4.1. Influence of elasticity

Consider a periodic four-layer spherical capsule of equal layer thickness $(r_j - r_{j-1})/r_1 = 1$, $j = 1, 4$ and alternately identical layers (1,3) and (2,4) subjected to the stepped dilatation profile ϑ_{p1} shown in 1. In this profile, the dilatation steps up from a

value of 0.1 in Layer 1 to 0.4 in Layer 4, simulating varying chemical concentrations in the layers. The elastic constants are taken to be $\lambda_1 = 35.7$, $\mu_1 = 10.3$, $l_1 = l_2 = -35.6$, $m_1 = -24.2$, and $n_1 = n_2 = -23.5$ kPa, where the third-order constants l and n are kept identical for all four layers and the second-order constants λ, μ and third-order constant m for Layer 2 (and Layer 4) are to be varied in the parametric study.

Fig. 7(a) and (b) plot $\lambda_2 - \mu_2 - m_2$ surfaces for constant values of u_r and T_r, respectively. The single point marked in each figure, where $\lambda_2 = \lambda_1$, $\mu_2 = \mu_1$ and $m_2 = m_1$, indicates a homogeneous sphere. Specifically, Fig. 7(a) plots the surfaces of constant u_r at the outermost boundary, i.e., $u_r(r = r_4)/r_1 = 1.5$, 2, 4. This reveals: (1) the λ_2, μ_2, m_2 values on the curved surfaces offer multiple choices of elastic constants for a targeted amount of swelling, (2) the bounds on λ_2, μ_2, m_2 can be determined if the displacement is to lie within or outside a certain range, (3) the surface shrinks with increasing swelling, which requires smaller values for λ_2, μ_2 (linearly compliant) but increasingly large negative values for m_2 (nonlinearly compliant), (4) larger swelling can, in general, be achieved by stronger layer dissimilarity, in contrast to the smaller swelling ($u_r(r = r_4)/r_1 = 1.372$) of the homogeneous sphere, (5) the third-order constant m_2, just as the second-order constants, can be effectively used to modify the swelling response, and (6) it becomes increasingly more difficult to achieve large swelling as the surfaces shrink and steepen with increasing outer displacement.

Fig. 7(b) shows the evolution of the $\lambda_2 - \mu_2 - m_2$ surfaces at the constant interfacial stress T_r at $r = r_2$, i.e., $T_r(r = r_2) = -5$, 0, 5 kPa. It is evident that: (1) there exists a zero stress curved surface which compartmentalizes the domain into tensile and compressive regions, (2) this compartmentalization may guide the selection of elastic constants yielding compressive stress to avoid interfacial delamination, or a small tensile stress to avoid compressive instability, and (3) the closer proximity of the surfaces representing zero and compressive stress implies a greater stress sensitivity to elastic parameter control in compression than in tension. The stress at the corresponding location in the homogeneous sphere is 3.87 kPa. Fig. 7(b) shows only the radial stress at $r = r_2$; the stresses throughout the capsule should be determined for the proper selection of elastic constants during biomaterial design.

In summary, Fig. 7 suggests the possibility of rationally designing for the elastic fields using second- and third-order elastic constants. The stress field has a crucial influence on the material integrity and the functionality of the composite, e.g., cell proliferation and orientation will likely be affected by the stress magnitude, sign and multiaxiality.

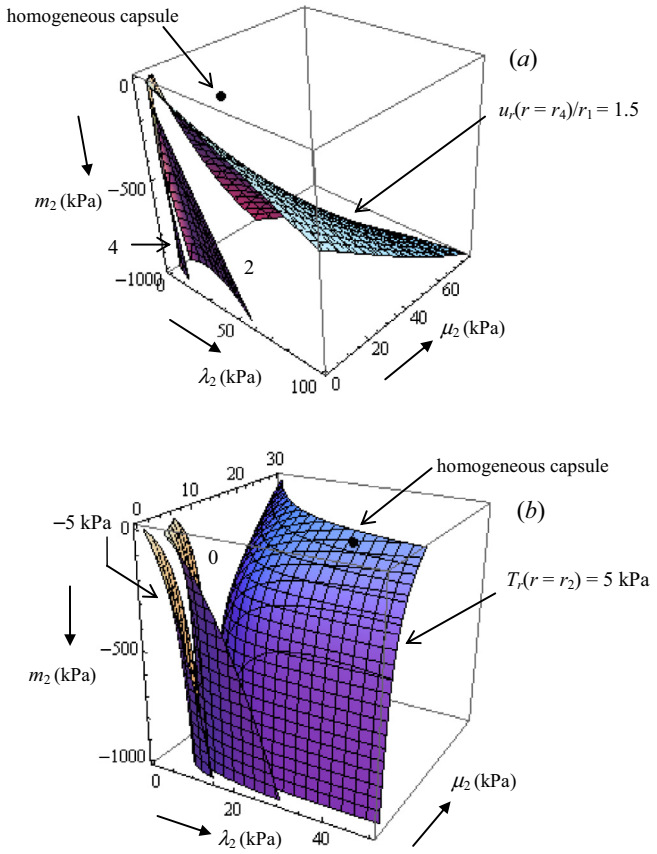

Fig. 7. The $\lambda_2 - \mu_2 - m_2$ surfaces of (a) constant radial displacement $u_r(r = r_4)/r_1 = 1.5$, 2, 4, and (b) constant radial stress $T_r(r = r_2) = -5$, 0, 5 kPa for a four-layer hydrogel composite subjected to the dilatation profile ϑ_{p1}. The fixed seven elastic constants are: $\lambda_1 = 35.7$ kPa, $\mu_1 = 10.3$ kPa, $l_1 = l_2 = -35.6$ kPa, $m_1 = -24.2$ kPa, and $n_1 = n_2 = -23.5$ kPa.

To further illustrate the influence of elastic dissimilarity, consider the four-layer sphere with Layers 1 and 3, and Layers 2 and 4, respectively identical in their elastic constants. The dilatation loading is ϑ_{p1}. Further, the constants for Layers 1 and 3 are selected as either $\lambda_1 = 35.7$, $\mu_1 = 10.3$, $l_1 = -35.6$, $m_1 = -24.2$ and $n_1 = -23.5$ kPa, or $\lambda_1 = 35.7$, $\mu_1 = 0.103$, $l_1 = -35.6$, $m_1 = -500$ and $n_1 = -23.5$ kPa. The elastic constants for Layers 2 and 4 are those that have been determined for the polymer gels (chosen from the data sets 18–34) through Eq. (30), and are listed explicitly in Table 3. From Fig. 8, it can be seen that the radial stress at $r = r_3$ varies from 1 to 9 kPa if the elastic constants for Layers 1 and 3 assume the first set of values and those for Layers 2 and 4 assume the values corresponding to the data sets listed in Table 3. If instead the constants for Layers 1 and 3 assume the second set of values (while the remaining layers have the constants listed in Table 3), the radial stresses are significantly different and can be compressive. Thus, Fig. 8 emphasizes the influence of elastic dissimilarity on the stress state.

4.2. Influence of interface positions

The effect of modifying the layer thicknesses of a four-layer composite, with Layers 1, 3 and Layers 2, 4 respectively identical, is next investigated. The chosen dilatation profile is ϑ_{p2}, where $\vartheta_1 = \vartheta_3 = 0.2$ and $\vartheta_2 = \vartheta_4 = 0.1$. Fig. 9 plots the variation of $u_r(r = r_4)/r_1$ vs. r_2 and r_3 ($>r_2$), holding r_1 and $r_4 = 4r_1$ fixed. The elastic constants employed are those for an agar-gelatain phantom, measured via the method of transient elastography (Catheline, Gennisson, & Fink, 2003; Gennisson et al., 2007): $\lambda_1 = 22.5 \times 10^6 = 100\lambda_2$, $\mu_1 = 80 = 100\mu_2$, $l_1 = l_2 = -2 \times 10^6$, $m_1 = -2 \times 10^6 = 0.01m_2$, $n_1 = n_2 = -100$ kPa. Layer 2 (or 4) is both linearly and nonlinearly more compliant than Layer 1 (or 3). Note the five to six orders difference in magnitude between λ and μ, and the four to six orders difference between n and l, m. That $\lambda \gg \mu$ shows that this material is nearly incompressible.

Fig. 9 shows that a maximum in u_r occurs at $r_2/r_1 \sim 1$ and $r_3/r_1 \sim 3.2$. The composite will appear like that indicated in Fig. 9, which shows the "near-elimination" of Layer 2. It suggests a competition between the effects of dilatation and material compliance. The dilatation in Layers 2 and 4 is half that in Layers 1 and 3, while the former are more compliant than the latter. Hence, for maximum u_r the size of Layers 2 and 4 should be reduced due to the dilatation effect, while they should be

Table 3
Elastic constants λ, μ and m obtained through Eq. (30), with $l = -35.6$ kPa and $n = -23.5$ kPa. The materials selected are those labeled in the first column.

No.	λ (kPa)	μ (kPa)	m (kPa)
18	40	39.83	−32.44
20	12.29	15.12	−30
21	5.00	85.47	−80.78
26	55.50	10.01	−30
28	10.15	50.50	−30
29	43.96	38.49	−60
30	55.91	4.10	−30
31	60	51.19	−100.82
32	60	12.21	−42.67
33	37.84	30.00	−39.87
34	21.86	60.00	−60.25

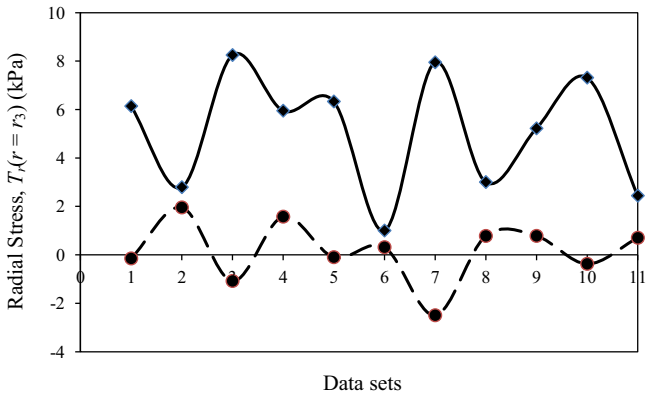

Fig. 8. Effect of elastic dissimilarity of four-layer spherical capsules on the interfacial radial stress at $r = r_3$. The elastic constants of the first and third layers represented by the solid line and dotted line are respectively: $\lambda = 35.7$, $\mu = 10.3$, $l = -35.6$, $m = -24.2$, $n = -23.5$ kPa, and $\lambda = 35.7$, $\mu = 0.103$, $l = -35.6$, $m = -500$, $n = -23.5$ kPa. The elastic constants of the second and fourth layers are taken from the data sets listed in Table 3.

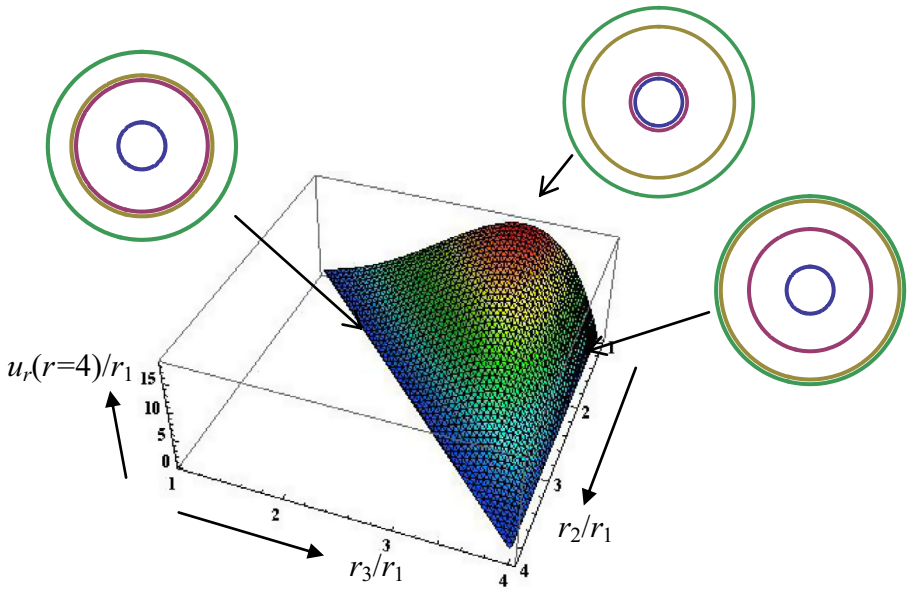

Fig. 9. Dependence of the surface displacement on r_2 and r_3 (r_1 and $r_4 = 4r_1$ held fixed) for a four-layer spherical composite subjected to the dilatation profile ϑ_{p2}. The elastic constants are: $\lambda_1 = 22.5 \times 10^6 = 100\lambda_2$, $\mu_1 = 80 = 100\mu_2$, $l_1 = l_2 = -2 \times 10^6$, $m_1 = -2 \times 10^6 = 0.01m_2$, $n_1 = n_2 = -100$ kPa. For maximum swelling elimination of Layer 2 is favored, while for very small swelling elimination of either Layer 3 or Layer 4 is favored.

increased due to the compliance effect. It turns out that the dilatation effect is more dominant for Layer 2 while the compliance effect is more dominant for Layer 4, resulting in a configuration with a much reduced size for Layer 2 and a fairly large size for Layer 4. In contrast, if a very small swelling of the composite is desired, Fig. 9 suggests that either r_3 should be just a little larger than r_2 (regardless of their values), or r_3 should be just a little less than r_4 (regardless of r_2). This implies the "near-elimination" of Layers 3 and 4, respectively, as also indicated in Fig. 9.

4.3. Influence of dilatation profile

It is also useful to investigate the influence of the chemical concentrations on the mechanical behavior. Two spherically symmetric dilatation profiles are selected for this investigation: ϑ_{p2} and ϑ_{p3}, where $r_1 = r_4/4 = r_3/3 = r_2/2$. The profile ϑ_{p3} is similar to ϑ_{p2}, with the dilatation values in the layers interchanged, i.e., $\vartheta_1 = \vartheta_3 = 0.1$ and $\vartheta_2 = \vartheta_4 = 0.2$. To eliminate the effect of material dissimilarity, a homogeneous sphere of radius r_4 is considered here with the following elastic constants: $\lambda = 35.7$, $\mu = 10.3$, $l = -35.6$, $m = -24.2$, and $n = -23.5$ kPa.

Fig. 10 plots the variation of (a) the radial displacement $u_r(r)/r_1$, (b) radial stress and (c) meridional stress against the radial coordinate r for the two dilatation profiles. It can be observed that even though the average dilatation value is the same for both profiles, the outer displacement (swelling) of the homogenous sphere subjected to ϑ_{p3} is ~30% larger than that subjected to ϑ_{p2}. The kinks in the displacement curves reflect the dilatation jumps at these locations. Moreover, ϑ_{p2} and ϑ_{p3} induce stresses which differ in sign. If the dilatation value at a certain radial location experiences a drop in value, then the surrounding regions experience a compressive radial stress, as at r_1 and r_3 when the profile is ϑ_{p2}, and at r_2 when it is ϑ_{p3}. The radial stress vanishes at the outermost boundary in both cases, as required by the boundary condition. Similar opposing meridional stress distributions are predicted for the two profiles. In addition, the meridional stress experiences discontinuities at the locations of the dilatation jumps.

The results in Fig. 10 show that the concentration profile in a multilayer capsule exerts a rather complex effect on the stress distributions. Coupled with dissimilarity in the layer elastic constants and thicknesses, the mechanical response is expected to be of even greater complexity. Hence, simulations with relatively simple nonlinear elastic models may provide useful qualitative and quantitative assessments which will aid the design of multilayer gels.

5. Discussion

The current work is motivated by prior results, e.g. Engler et al. (2006), Marklein and Burdick (2010), Kloxin et al. (2010), and Bajaj et al. (2010), which show that the mechanical properties of the bioenvironment have a profound influence on the biological processes occurring in it. It highlights the importance of nonlinear elasticity in the mechanical modeling of both synthetic and bio-polymer gels. There exist many nonlinear models for soft matter, e.g., microscopic models based on internal structural/chemical variables or molecular dynamics simulations, and macroscopic models derived from the

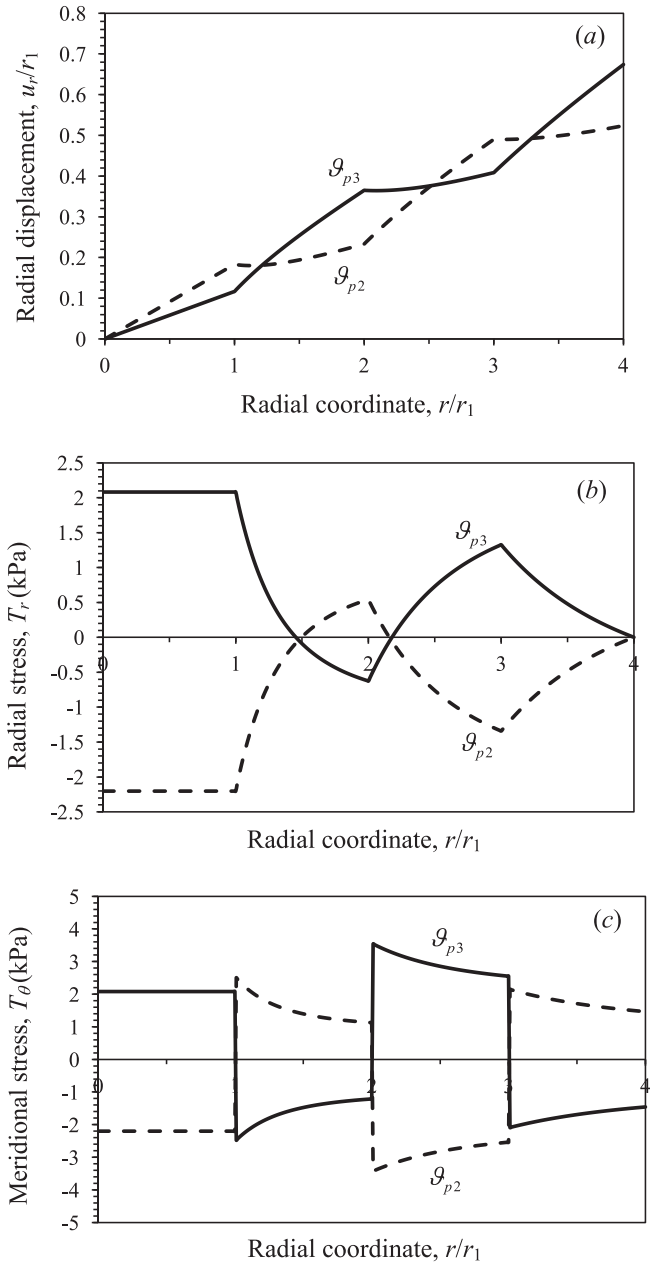

Fig. 10. Variation of the (a) normalized radial displacement, (b) radial stress and (c) meridional stress with normalized radial coordinate r/r_1 in a homogeneous sphere subjected to the dilatation profiles ϑ_{p2} and ϑ_{p3}.

phenomenology of the nonlinear behavior (Wu, 2011). Microscopic models are generally used for investigating the internal structure and its dynamics, but may be computationally prohibitive if the desired outputs are to be macroscopic variables. Although multiscale models that aim to bridge the microscopic and the macroscopic have been developed, simple phenomenological models can be used to study the response of architecturally complex gels (multiple layers with different elastic properties) without significant computational cost. This is demonstrated in this work, which shows that solutions can be obtained for an *N*-layer composite gel.

The second-order elastic model requiring five elastic constants is generic and describes a typical weakly/moderately nonlinear elastic material. The five constants can be obtained indirectly through fitting the relevant equations to experimental data, or directly through measurements. Acousto-elastic methods have been used to determine the elastic constants of soft gels (Catheline et al., 2003; Gennisson et al., 2007). The constants used in the simulations of Fig. 9 were directly determined via such methods in the framework of second-order elasticity. Atomic force microscopic methods have also been used to

study the mechanical properties of cross-linked polyelectrolyte multilayer films in which the Young's modulus was usually the only elastic parameter determined (Richert, Engler, Discher, & Picart, 2004). However, much research remains to be done on the relationship between the elastic constants, especially the higher-order ones, and the biological parameters, e.g., the dependence of cell differentiation and growth characteristics on the third-order elastic constants. The current work predicts the mechanical state for a given bioenvironment, but the link of the mechanical state to the biological activities is not yet established. The interface between mechanics and biology remains an interesting challenge.

The solutions for the stresses and displacements in an arbitrary N-layer cylindrical and spherical gel have been obtained for constant stepped dilatations. The problem can be extended to other loading and boundary conditions. For instance, Eqs. (13)–(16) can be solved analytically for non-constant dilatations within the layers and for pressure loading on the outer/inner surfaces. For a more general shape other than spherical or cylindrical, the second-order elastic model can be incorporated as a constitutive model in a numerical strategy to solve complex boundary-value problems.

Naturally, the current model has its limits. It does not consider time and rate dependence phenomena such as viscoelasticity and how they may modulate the mechanical state over time. Detailed theoretical models accounting for finite viscosity, plasticity and rate effects have been developed (El Sayed, Mota, Fraternali, & Ortiz, 2008) and the visco-elasto-plastic effects have been probed experimentally via indentation methods (Constantinides, Kalcioglu, McFarland, Smith, & Van Vliet, 2008). Factors such as the elastic anisotropy of the soft materials, e.g., biological tissues with aligned fibers, have often been ignored. It is however, possible to account for elastic anisotropy through the use of additional strain invariants in the strain energy functions (Destrade et al., 2010). The modeling of the anisotropic viscoelasticity of soft tissues for medical image computing has also been attempted (Taylor et al., 2009).

6. Concluding remarks

In this paper, power-law solutions for the stresses and displacements in multilayer spherical and cylindrical gels subjected to stepped dilatations are developed in the framework of second-order elasticity. This requires the use of five elastic constants for each layer. It is shown that universal relations can be derived for uniaxial tension and the swelling of the gels due to the effect of pH. Reasonably good fit of these universal relations to experimental data has been obtained for a wide range of synthetic and biological gels. The importance of elastic nonlinearity in the mechanical behavior of such gels is emphasized.

Further simulations for a four-layer composite show that dissimilarity in the layer elasticities, thicknesses and dilatations can strongly influence the mechanical response. Consequently, the biomaterial design may benefit from such simulations, which can be used to search for the loading, geometrical and material parameters most suitable for a desired mechanical state in a specific application. This may enable multiple functionalities, enhance material integrity and improve the biomimicry.

References

Bajaj, P., Tang, X., Saif, T. A., & Bashir, R. (2010). Stiffness of the substrate influences the phenotype of embryonic chicken cardiac myocytes. *Journal of Biomedical Materials Research Part A, 95A*, 1261–1269.

Balzani, D., Neff, P., Schroder, J., & Holzapfel, G. A. (2006). A polyconvex framework for soft biological tissues. Adjustment to experimental data. *International Journal of Solids and Structures, 43*, 6052–6070.

Batich, C. D., Jun, Y., Bucaria, C., & Elsabee, M. (1993). Swelling behavior of pH-sensitive copolymers based on styrene and 4-(or 2-)vinylpyridine. *Macromolecules, 26*, 4675–4680.

Catheline, S., Gennisson, J. L., & Fink, M. (2003). Measurement of elastic nonlinearity of soft solid with transient elastography. *Journal of the Acoustical Society of America, 114*, 3087–3091.

Constantinides, G., Kalcioglu, Z. I., McFarland, M., Smith, J. F., & Van Vliet, K. J. (2008). Probing mechanical properties of fully hydrated gels and biological tissues. *Journal of Biomechanics, 41*, 3285–3289.

Cortez, C., Tomaskovic-Crook, E., Johnston, A. P. R., Radt, B., Cody, S. H., Scott, A. M., et al (2006). Targeting and uptake of multilayered particles to colorectal cancer cells. *Advanced Materials, 18*, 1998–2003.

Destrade, M., Gilchrist, M. D., & Ogden, R. W. (2010). Third- and fourth-order elasticities of biological soft tissues. *Journal of the Acoustical Society of America, 127*, 2103–2106.

Detzel, C. J., Larkin, A. L., & Rajagopalan, P. (2011). Polyelectrolyte multilayers in tissue engineering. *Tissue Engineering Part B-Reviews, 17*, 101–113.

Dobrynin, A. V., & Carrillo, J. M. Y. (2011). Universality in nonlinear elasticity of biological and polymeric networks and gels. *Macromolecules, 44*, 140–146.

El Sayed, T., Mota, A., Fraternali, F., & Ortiz, M. (2008). A variational constitutive model for soft biological tissues. *Journal of Biomechanics, 41*, 1458–1466.

Engler, A. J., Sen, S., Sweeney, H. L., & Discher, D. E. (2006). Matrix elasticity directs stem cell lineage specification. *Cell, 126*, 677–689.

Facca, S., Cortez, C., Mendoza-Palomares, C., Messadeq, N., Dierich, A., Johnston, A. P. R., et al (2010). Active multilayered capsules for in vivo bone formation. *Proceedings of the National Academy of Sciences of the United States of America, 107*, 3406–3411.

Gennisson, J. L., Renier, M., Catheline, S., Barriere, C., Bercoff, J., Tanter, M., et al (2007). Acoustoelasticity in soft solids: Assessment of the nonlinear shear modulus with the acoustic radiation force. *Journal of the Acoustical Society of America, 122*, 3211–3219.

Goriely, A., & Ben Amar, M. (2005). Differential growth and instability in elastic shells. *Physical Review Letters, 94*, 198103.

Hamilton, M. F., Ilinskii, Y. A., & Zabolotskaya, E. A. (2004). Separation of compressibility and shear deformation in the elastic energy density (L). *Journal of the Acoustical Society of America, 116*, 41–44.

Johnson, L. M., DeForest, C. A., Pendurti, A., Anseth, K. S., & Bowman, C. N. (2010). Formation of three-dimensional hydrogel multilayers using enzyme-mediated redox chain initiation. *ACS Applied Materials & Interfaces, 2*, 1963–1972.

Johnston, A. P. R., Cortez, C., Angelatos, A. S., & Caruso, F. (2006). Layer-by-layer engineered capsules and their applications. *Current Opinion in Colloid & Interface Science, 11*, 203–209.

Kloxin, A. M., Benton, J. A., & Anseth, K. S. (2010). In situ elasticity modulation with dynamic substrates to direct cell phenotype. *Biomaterials, 31*, 1–8.

Li, P., Kim, N. H., Siddaramaiah & Lee, J. H. (2009). Swelling behavior of polyacrylamide/laponite clay nanocomposite hydrogels: pH-sensitive property. *Composites Part B-Engineering, 40*, 275–283.

Macklin, P., & Lowengrub, J. (2007). Nonlinear simulation of the effect of microenvironment on tumor growth. *Journal of Theoretical Biology, 245*, 677–704.
Marklein, R. A., & Burdick, J. A. (2010). Spatially controlled hydrogel mechanics to modulate stem cell interactions. *Soft Matter, 6*, 136–143.
Motonaga, T., & Shibayama, M. (2001). Studies on pH and temperature dependence of the dynamics and heterogeneities in poly(N-isopropylacrylamide-co-sodium acrylate) gels. *Polymer, 42*, 8925–8934.
Murnaghan, F. D. (1951). *Finite deformation of an elastic solid*. New York: John Wiley.
Naficy, S., Razal, J. M., Whitten, P. G., Wallace, G. G., & Spinks, G. M. (2012). A pH-sensitive, strong double-network hydrogel: Poly(ethylene glycol) methyl ether methacrylates–poly(acrylic acid). *Journal of Polymer Science Part B: Polymer Physics, 50*, 423–430.
Philippova, O. E., Hourdet, D., Audebert, R., & Khokhlov, A. R. (1997). PH-responsive gels of hydrophobically modified poly(acrylic acid). *Macromolecules, 30*, 8278–8285.
Richert, L., Engler, A. J., Discher, D. E., & Picart, C. (2004). Elasticity of native and cross-linked polyelectrolyte multilayer films. *Biomacromolecules, 5*, 1908–1916.
Shibayama, M., Ikkai, F., Inamoto, S., Nomura, S., & Han, C. C. (1996). PH and salt concentration dependence of the microstructure of poly(N-isopropylacrylamide-co-acrylic acid) gels. *Journal of Chemical Physics, 105*, 4358–4366.
Storm, C., Pastore, J. J., MacKintosh, F. C., Lubensky, T. C., & Janmey, P. A. (2005). Nonlinear elasticity in biological gels. *Nature, 435*, 191–194.
Tang, J. M., Tung, M. A., Lelievre, J., & Zeng, Y. Y. (1997). Stress–strain relationships for gellan gels in tension, compression and torsion. *Journal of Food Engineering, 31*, 511–529.
Taylor, Z. A., Comas, O., Cheng, M., Passenger, J., Hawkes, D. J., Atkinson, D., et al (2009). On modelling of anisotropic viscoelasticity for soft tissue simulation: numerical solution and GPU execution. *Medical Image Analysis, 13*, 234–244.
Teramura, Y., Kaneda, Y., & Iwata, H. (2007). Islet-encapsulation in ultra-thin layer-by-layer membranes of poly(vinyl alcohol) anchored to poly(ethylene glycol)-lipids in the cell membrane. *Biomaterials, 28*, 4818–4825.
Urayama, K., Ogasawara, S., & Takigawa, T. (2006). Pure shear deformation of physical and chemical gels of poly(vinyl alcohol). *Polymer, 47*, 6868–6873.
Wang, M., & Hill, R. J. (2008). Electric-field-induced displacement of charged spherical colloids in compressible hydrogels. *Soft Matter, 4*, 1048–1058.
Wang, D., & Wu, M. S. (2013). Analytical solutions for bilayered spherical hydrogel subjected to constant dilatation. *Mechanics of Materials, 58*, 12–22.
Wen, Q., Basu, A., Janmey, P. A., & Yodh, A. G. (2012). Non-affine deformations in polymer hydrogels. *Soft Matter, 8*, 8039–8049.
Williams, S. R., Mather, B. D., Miller, K. M., & Long, T. E. (2007). Novel Michael addition networks containing urethane hydrogen bonding. *Journal of Polymer Science Part A-Polymer Chemistry, 45*, 4118–4128.
Wu, M. S. (2011). Strategies and challenges for the mechanical modeling of biological and bio-inspired materials. *Materials Science and Engineering: C, 31*, 1209–1220.
Wu, M. S., & Kirchner, H. O. K. (2010). Nonlinear elasticity modeling of biogels. *Journal of the Mechanics and Physics of Solids, 58*, 300–310.
Wu, M. S., & Kirchner, H. O. K. (2011). Second-order elastic solutions for spherical gels subjected to spherically symmetric dilatation. *Mechanics of Materials, 43*, 721–729.
Yohsuke, B., Urayama, K., Takigawa, T., & Ito, K. (2011). Biaxial strain testing of extremely soft polymer gels. *Soft Matter, 7*, 2632–2638.
Zhang, J., & Peppas, N. A. (2000). Synthesis and characterization of pH- and temperature-sensitive poly(methacrylic acid)/poly(N-isopropylacrylamide) interpenetrating polymeric networks. *Macromolecules, 33*, 102–107.